

ReZero: Boosting MCTS-based Algorithms by Backward-view and Entire-buffer Reanalyze

Anonymous Author(s)

Affiliation

Address

email

Abstract: Monte Carlo Tree Search (MCTS)-based algorithms, such as MuZero and its derivatives, have achieved widespread success in various decision-making domains. These algorithms employ the *reanalyze* process to enhance sample efficiency from stale data, albeit at the expense of significant wall-clock time consumption. To address this issue, we propose a general approach named ReZero to boost tree search operations for MCTS-based algorithms. Specifically, drawing inspiration from the one-armed bandit model, we reanalyze training samples through a backward-view reuse technique which uses the value estimation of a certain child node to save the corresponding sub-tree search time. To further adapt to this design, we periodically reanalyze the entire buffer instead of frequently reanalyzing the mini-batch. The synergy of these two designs can significantly reduce the search cost and meanwhile guarantee or even improve performance. Experiments conducted on Atari environments, DMControl suites and board games demonstrate that ReZero substantially improves training speed while maintaining high sample efficiency.

Keywords: Deep Reinforcement Learning, Monte Carlo tree search, MuZero, information reuse, reanalyze

1 Introduction

Within the field of model-based Reinforcement Learning (RL) [1, 2], Monte Carlo Tree Search (MCTS) [3] has been proven to be a efficient method for utilizing models for planning. It incorporates the UCB1 algorithm [4] into the tree search process and has achieved promising results in a wide range of scenarios. Specifically, AlphaZero [5] plays a big role in combining deep reinforcement learning with MCTS, achieving notable accomplishments that can beat top-level human players. While it can only be applied to environments with perfect simulators, MuZero [6] extended the algorithm to cases without known environment models, resulting in good performance in a wider range of tasks. Following MuZero, many successor algorithms have emerged, enabling MuZero to be applied in continuous action spaces [7], offline training scenarios [8], and etc. All these MCTS-based algorithms made valuable contributions to the universal applicability of the MCTS+RL paradigm.

However, the extensive tree search computations incur additional time overhead for these algorithms: During the data collection phase, the agent needs to execute MCTS to select an action every time it receives a new state. Furthermore, due to the characteristics of tree search, it is challenging to parallelize it using commonly used vectorized environments [9], further amplifying the speed disadvantage. On the other hand, during the reanalyze [8] process, in order to obtain higher-quality update targets, the latest models are used to re-run MCTS on the training mini-batch. The wall-clock time thus increases as a trade-off for high sample efficiency. The excessive cost has become a bottleneck hindering the further promotion of these algorithms.

38 Recently, a segment of research endeavors is directed toward mitigating the above wall-clock time
 39 overhead. On the one hand, SpeedyZero [10] diminishes algorithms’ time overheads by deploying
 40 a parallel execution training pipeline; however, it demands additional computational resources. On
 41 the other hand, it remains imperative to identify methodologies that accelerate these algorithms
 42 without imposing extra demands. PTSAZero [11], for instance, compresses the search space via
 43 state abstraction, decreasing the time cost per search. In contrast, we aim to adopt a method that
 44 is orthogonal to both of the previous approaches. It does not require state space compression but
 45 directly reduces the search space through value estimation, and it does not introduce additional
 46 hardware overhead.

47 In this paper, we introduce ReZero, a new approach/framework designed to boost the MCTS-based
 48 algorithms. Firstly, inspired by the one-armed bandit model [12], we propose a backward-view rean-
 49alyze technique that proceeds in the reverse direction of the trajectories, utilizing previously searched
 50 root values to bypass the exploration of specific child nodes, thereby saving time. Additionally, we
 51 have proven the convergence of our search mechanism based on the non-stationary bandit model,
 52 i.e., the distribution of child node visits will concentrate on the optimal node. Secondly, to better
 53 adapt to our proposed backward-view reanalyze technique, we have devised a novel pipeline that
 54 concentrates MCTS calls within the reanalyze process and periodically reanalyzes the entire buffer
 55 after a fixed number of training iterations. This entire-buffer reanalyze not only reduces the number
 56 of MCTS calls but also better leverages the speed advantages of parallelization. Skipping the search
 57 of specific child nodes can be seen as a pruning operation, which is common in different tree search
 58 settings. Reanalyze is also a common module in MCTS-based algorithms. Therefore, our algorithm
 59 design is universal and can be easily applied to the MCTS-based algorithm family. In addition,
 60 it will not bring about any overhead in computation resources. Empirical experiments (Section 5)
 61 show that our approach yields good results in both single-agent discrete-action environments (Atari
 62 [13]), two-player board games [14], and continuous control suites [15], greatly improving the train-
 63ing speed while maintaining or even improving sample efficiency. The main contributions of this
 64 paper can be summarized as follows:

- 65 • We design a method to speed up a single tree search by the backward-view reanalyze technique.
 66 Theoretical support for the convergence of our proposed method is also provided.
- 67 • We propose an efficient framework with the entire-buffer reanalyze mechanism that further re-
 68duces the number of MCTS and enhance its parallelization, boosting MCTS-based algorithms.
- 69 • We conduct experiments on diverse environments and investigate ReZero through ablations.

70 2 Related Work

71 Recent research has focused on accelerating MCTS-based algorithms[14, 5, 6, 16, 7, 17, 8, 18].
 72 Mei et al. [10] reduces the algorithm’s time overhead by designing a parallel system; however, this
 73 method requires more computational resources and involves some adjustments for large batch train-
 74ing. Fu et al. [11] narrows the search space through state abstraction, which amalgamates redundant
 75 information, thereby reducing the time cost per search. KataGo [19] use a naive information reuse
 76 trick. They save sub-trees of the search tree and serve as initialization for the next search. How-
 77ever, our proposed backward-view reanalyze technique is fundamentally different from this naive
 78 forward-view reuse and can enhance search results while saving time. To our knowledge, we are
 79 the first to enhance MCTS by reusing information in a backward-view. Our proposed approach
 80 can seamlessly integrate with various MCTS-based algorithms, many of which [10, 11, 18, 20] are
 81 orthogonal to our contributions.

82 3 Preliminaries

83 3.1 MuZero

84 MuZero [6] is a fundamental model-based RL algorithm that incorporates a value-equivalent model
 85 [21] and leverages MCTS for planning within a learned latent space. The model consists of three
 86 core components: a *representation* model h_θ , a *dynamics* model g_θ , and a *prediction* model f_θ :

$$\begin{aligned}
\text{Representation:} \quad & s_t = h_\theta(o_{t-l:t}) \\
\text{Dynamics:} \quad & s_{t+1}, r_t = g_\theta(s_t, a_t) \\
\text{Prediction:} \quad & v_t, p_t = f_\theta(s_t)
\end{aligned} \tag{1}$$

87

88 The representation model transforms last observation sequences $o_{t-l:t}$ into a corresponding latent
89 state s_t . The dynamics model processes this latent state alongside an action a_t , yielding the next
90 latent state s_{t+1} and an estimated reward r_t . Finally, the prediction model accepts a latent state and
91 produces both the predicted policy p_t and the state’s value v_t . These outputs are instrumental in
92 guiding the agent’s action selection throughout its MCTS. Lastly the agent samples the best action
93 a_t following the searched visit count distribution. Refer to Appendix C for more details on MuZero
94 during the training and inference phases.

95 3.2 Bandit-view Tree Search

96 A stochastic bandit has K arms, and playing each arm means sampling a reward from the corre-
97 sponding distribution. For a search tree in MCTS, the root node can be seen as a bandit, with each
98 child node as an arm. The left side of Figure 1 illustrates this idea. However, as the policy is contin-
99 uously improved during the search process, the reward distribution for the arms should change over
100 time. Therefore, UCT [22] modeled the root node as a non-stationary stochastic bandit with a drift
101 condition:

$$\mathbb{P}(\hat{\mu}_{is} - \mu_i \geq \varepsilon) \leq \exp(-\frac{\varepsilon^2 s}{C^2}) \text{ and } \mathbb{P}(\hat{\mu}_{is} - \mu_i \leq -\varepsilon) \leq \exp(-\frac{\varepsilon^2 s}{C^2}) \tag{2}$$

102 Where $\hat{\mu}_{is}$ is the average reward of the first s samples of arm i . μ_i is the limit of $\mathbb{E}[\hat{\mu}_{is}]$ as s
103 approaches infinity, which indicates that the expectation of the node value converges. C is an appro-
104 priate constant characterizes the rate of concentration.

105 Based on this modeling, UCT uses the bandit algorithm UCB1 [4] to select child nodes. AlphaZero
106 inherits this concept and employs a variant formula:

$$UCB_{score}(s, a) = Q(s, a) + cP(s, a) \frac{\sqrt{\sum_b N(s, b)}}{1 + N(s, a)} \tag{3}$$

107 where s is the state corresponding to the current node, a is the action corresponding to a child node.
108 $Q(s, a)$ is the mean return of choosing action a , $P(s, a)$ is the prior score of action a , $N(s, a)$ is the
109 total time that a has been chosen, $\sum_b N(s, b)$ is the total time that s has been visited. Viewing tree
110 search from the bandit-view inspired us to use techniques from the field of bandits to improve the
111 tree search. In next section, We use the idea of the one-armed bandit model to design our algorithm
112 and prove the convergence of our algorithm based on the non-stationary bandit model.

113 4 Method

114 4.1 Backward-view Reanalyze

115 Our algorithm design stems from a simple inspiration: if we could know the true state-value (e.g.,
116 expected long-term return) of a child node in advance, we could save the search for it, thus con-
117 serving search time. As shown on the right side of Figure 1, we directly use the true expectation
118 μ_A to evaluate the quality of Arm A, thereby eliminating the need for the back-propagated value to
119 calculate the score in Eq. 3. This results in the process occurring within the gray box in Figure 1
120 being omitted. Indeed, this situation can be well modeled as an **one-armed bandit** [12], which also
121 facilitates our subsequent theoretical analysis.

122 Driven by the aforementioned motivation, we aspire to obtain the expected return of a child node
123 in advance. However, the true value is always unknown. Consequently, we resort to using the root
124 value obtained from MCTS as an approximate substitute. Specifically¹, for two adjacent time steps

¹The subscript denotes the trajectory, the superscript denotes the time step in the trajectory.

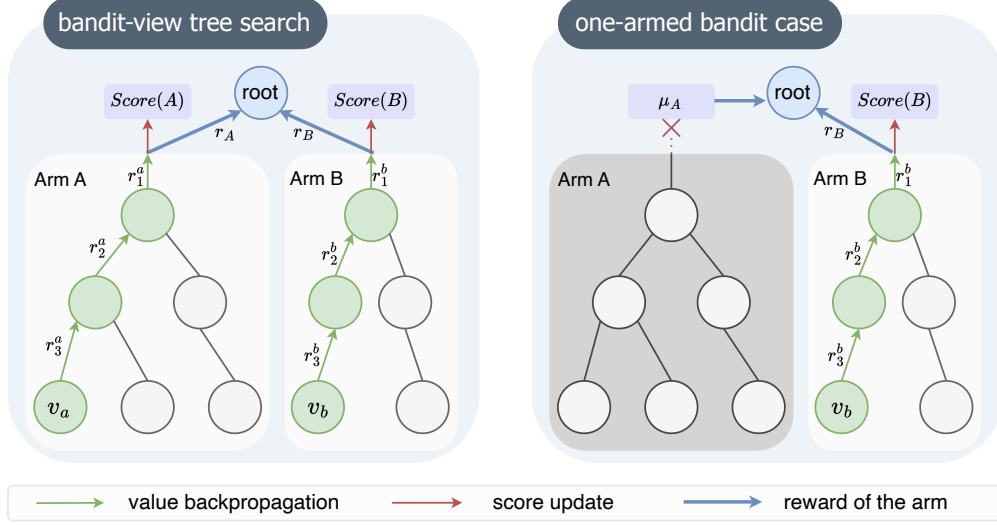


Figure 1: The connection between MCTS and bandits. **Left** shows tree search in a bandit-view. When the action A is selected, a return r_A will be returned, where $r_A = \sum_{t=1}^3 \gamma^{t-1} r_t^a + \gamma^3 v_a$. For the root node, the traversal, evaluation and back-propagation occurring in the sub-tree can be approximated as sampling from an non-stationary distribution. Thus it can be seen as a non-stationary bandit. **Right** shows the one-armed bandit case. Once the true value μ_A is known, we can evaluate arm A using μ_A , thereby eliminating the need to rely on subsequent tree search processes.

125 S_0^1 and S_0^0 in Figure 2, when searching for state S_0^1 , the root node corresponds to a child node of
 126 S_0^0 . Therefore, the root value obtained can be utilized to assist the search for S_0^0 . However, there is
 127 a temporal contradiction. S_0^1 is the successor state of S_0^0 , yet we need to complete the search for S_0^1
 128 first. Fortunately, this is possible during the reanalyze process.

129 During reanalyze, since the trajectories were already collected in the replay buffer, we can perform
 130 tree search in a backward-view, which searches the trajectory in a reverse order. Figure 2 illustrates a
 131 batch containing $n + 1$ trajectories, each of length $k + 1$, and S_l^t is the t -th state in the l -th trajectory.
 132 We first conduct a search for all S_l^k s, followed by a search for all S_l^{k-1} s, and so on. After we search
 133 on state S_l^{t+1} , the root value m_l^{t+1} is obtained.² When engaging in search on S_l^t , we assign the
 134 value of S_l^{t+1} to the fixed value m_l^{t+1} . During traverse in the tree, we select the action a_{root} for root
 135 node S_l^t with the following equation:

$$a_{root} = \arg \max_a I_l^t(a) \quad (4)$$

136

$$I_l^t(a) = \begin{cases} UCB_{score}(S_l^t, a), & a \neq a_l^t \\ r_l^t + \gamma m_l^{t+1}, & a = a_l^t \end{cases} \quad (5)$$

137 where a refers to the action associated with a child node, a_l^t is the action corresponding to S_l^{t+1} ,
 138 and r_l^t signifies the reward predicted by the dynamic model. If an action distinct from a_l^t is selected,
 139 the simulation continues its traversal with the original setting as in MuZero. *If action a_l^t is selected,*
 140 *this simulation is terminated immediately.* Since the time used to search for node S_l^{t+1} is saved, this
 141 enhanced search process is faster than the original version. Algorithm 1 shows the specific design
 142 with Python-like code.³

²To facilitate the explanation, we have omitted details such as the latent space and do not make a deliberate distinction between states and nodes.

³Our enhanced search process is implemented through `reuse_MCTS()`, where `select_root_child()` performs the action selection method of Equation 5. The `traverse()` and `backpropagate()` represent the forward search and backward propagation processes in standard MCTS.

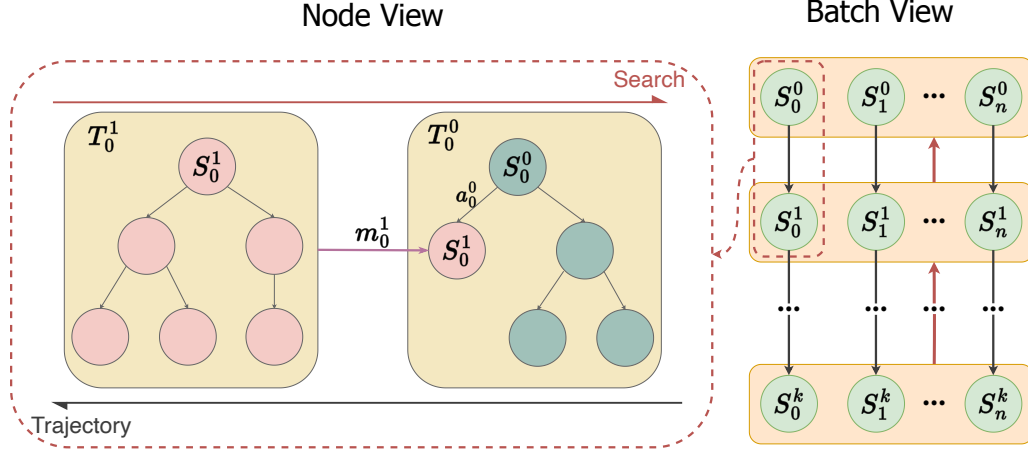


Figure 2: An illustration about the backward-view reanalyze in node and batch view. We sample $n + 1$ trajectories of length $k + 1$ to form a batch and conduct the search in the reverse direction of trajectories. From the node view, we would first search S_0^1 and then pass root value m_0^1 to S_0^0 to evaluate the value of a child node. T_0^1 and T_0^0 are the corresponding search trees. From the batch view, we would group all S^1 s into a sub batch to search together and pass the root values to the S^0 s.

Algorithm 1 Python-like code for information reuse

```
# trajectory_segment: a segment with length K
def search_backwards(trajectory_segment):
    # prepare search context from the segment
    roots, actions = prepare(trajectory_segment)
    policy_targets = []
    # search the roots backwards
    for i in range(K, 1, -1):
        if i == K:
            # origin MCTS for Kth root
            policy, value = origin_MCTS(roots[i])
        else:
            # reuse information from previous search
            policy, value = reuse_MCTS(
                roots[i], actions[i], value
            )
        policy_targets.append(policy)

# N: simulation numbers during one search
def reuse_MCTS(root, action, values):
    for i in range(N):
        # select an action for root node
        a = select_root_child(root, action, value):
        # early stop the simulation
        if a == action:
            backpropagate()
            break
        # traverse to the leaf node
    else:
        traverse()
        backpropagate()
```

143 4.2 Theoretical Analysis

144 AlphaZero selects child nodes using Equation 3 and takes the final action based on the visit counts.
 145 In the previous section, we replace Equation 3 with Equation 5, which undoubtedly impacts the
 146 visit distribution of child nodes. Additionally, since we use the root value as an approximation to
 147 true expectation, the error between the two may also affect the search results. To demonstrate the
 148 reliability of our algorithm, in this section, we model the root node as a non-stationary bandit and
 149 prove that, as the number of total visit increases, the visit distribution gradually concentrates on the
 150 optimal arm. Specifically, we have the following theorem:

151 **Theorem 1** For a non-stationary bandit that conforms to the assumptions of Equation 2, denote
 152 the total number of rounds as n , the prior score for arm i as P_i , and the number of times a sub-
 153 optimal arm i is selected in n rounds as $T_i(n)$, then use a sampled estimation instead of UCB value
 154 to evaluate a specific arm (like we do in Equation 5) can ensure that $\frac{\mathbb{E}[T_i(n)]}{n} \rightarrow 0$ as $n \rightarrow \infty$.
 155 Specifically, if we know the n times sample mean $\hat{\mu}^*$ of the optimal arm in advance, then $\mathbb{E}[T_i(n)]$
 156 for all sub-optimal arm i satisfies

$$\mathbb{E}[T_i(n)] \leq 2 + \frac{2P_i\sqrt{n-1}}{\Delta_i - \varepsilon} + \frac{C^2}{(\Delta_i - \varepsilon)^2} + n \exp\left(-\frac{n\varepsilon^2}{C^2}\right) \quad (6)$$

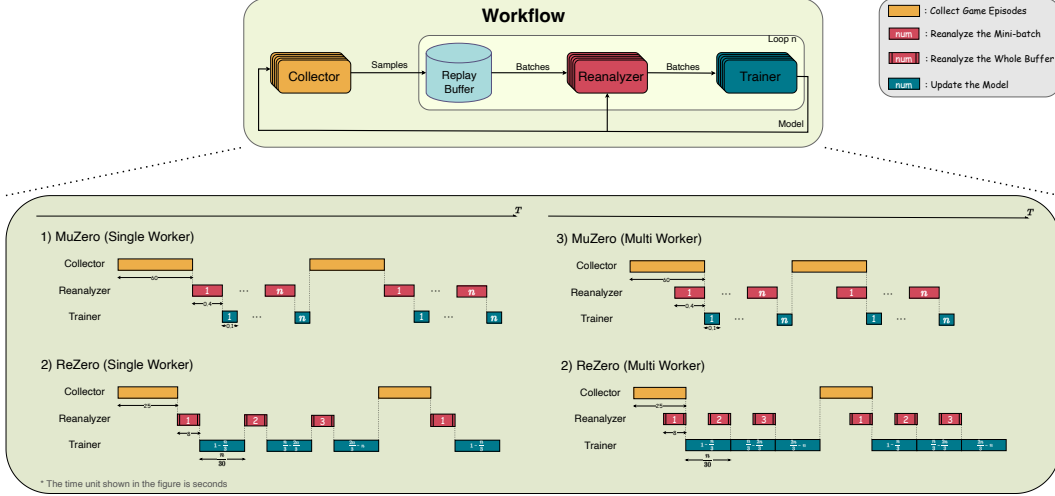


Figure 3: Execution workflow and runtime cycle graph about MuZero and ReZero in both single and multiple worker cases. The number inside the modules represent the number of iterations, and the number under the modules represent the time required for module execution. The model is updated n iterations between two collections. MuZero reanalyzes the mini-batch before each model update. ReZero reanalyzes the entire buffer after certain iterations ($\frac{n}{3}$ for example), which not only reduces the total number of MCTS calls, but also takes advantage of the processing speed of large batches.

157 Otherwise, if we have the n times sample mean $\hat{\mu}_l$ of a sub-optimal arm l , then for arm l ,

$$\mathbb{E}[T_l(n)] \leq 1 + \frac{2C^6}{\varepsilon^4 P_1^2} + n \exp\left(-\frac{n(\Delta_l - \varepsilon)^2}{C^2}\right) \quad (7)$$

158 and for other sub-optimal arms,

$$\mathbb{E}[T_i(n)] \leq 3 + \frac{2P_i \sqrt{n-1}}{\Delta_i - \varepsilon} + \frac{C^2}{(\Delta_i - \varepsilon)^2} + \frac{2C^6}{\varepsilon^4 P_1^2} \quad (8)$$

159 where Δ_i is the optimal gap for arm i , ε is a constant in $(0, \Delta_i)$, and C is the constant in Eq. 2.

160 We offer a complete proof and explanations in Appendix A and draw similar conclusions for Alp-
 161 haZero, which shows that our method has a lower upper bound for $\mathbb{E}[T_i(n)]$. This implies that our
 162 algorithm may yield a visit distribution more concentrated on the optimal arm. This is a potential
 163 worth exploring in future work, especially in offline scenarios [8] where reanalyze becomes the sole
 164 method for policy improvement.

165 4.3 The ReZero Framework

166 The technique introduced in Section 4.1 will bring a new problem in practice. The experiments in
 167 the Appendix B.3 demonstrate that batching MCTS allows for parallel model inference and data
 168 processing, thereby accelerating the average search speed. However, as shown in the Figure 2, to
 169 conduct the backward-view reanalyze, we need to divide the batch into $\frac{1}{k+1}$ of its original size. This
 170 diminishes the benefits of parallelized search and, on the contrary, makes the algorithm slower.

171 We propose a new pipeline that is more compatible with the method introduced in Section 4.1.
 172 In particular, during the collect phase, we have transitioned from using MCTS to select actions to
 173 directly sampling actions based on the policy network’s output. This shift can be interpreted as an
 174 alternative method to augment exploration in the collect phase, akin to the noise injection at the
 175 root node in MCTS-based algorithms. Figure 6b in Appendix B.3 indicates that this modification
 176 does not significantly compromise performance during evaluation. For the reanalyze process, we
 177 introduce the periodical entire-buffer reanalyze. As shown in Figure 3, we reanalyze the whole
 178 buffer after a fixed number of training iterations. For each iteration, we do not need to run MCTS to
 179 reanalyze the mini-batch, only need to sample the mini-batch and execute the gradient descent.

Overall, this design offers two significant advantages: ① The entire buffer reanalyze is akin to the fixed target net mechanism in DQN [23], maintaining a constant policy target for a certain number of training iterations. Reducing the frequency of policy target updates correspondingly decreases the number of MCTS calls. Concurrently, this does not result in a decrease in performance. ② Since we no longer invoke MCTS during the collect phase, all MCTS calls are concentrated in the reanalyze process. And during the entire-buffer reanalyze, we are no longer constrained by the size of the mini-batch, allowing us to freely adjust the batch size to leverage the advantages of large batches. Figure 6c shows both excessively large and excessively small batch sizes can lead to a decrease in search speed. We choose the batch size of 2000 according to the experiment in Appendix B.3.

Experiments show that our algorithm maintains high sample efficiency and greatly save the running time of the algorithm. Our pipeline also has the following potential improvement directions:

- When directly using policy for data collection, action selection is no longer bound by tree search. Thus, previous vectorized environments like Weng et al. [9] can be seamlessly integrated. Besides, this design makes MCTS-based algorithms compatible with existing RL exploration methods like Badia et al. [24].
- Our method no longer needs to reanalyze the mini-batch for each iteration, thus decoupling the process of *reanalyze* and *training*. This provides greater scope for parallelization. In the case of multiple workers, we can design efficient parallelization paradigms as shown in Figure 3.
- We can use a more reasonable way, such as weighted sampling to preferentially reanalyze a part of the samples in the buffer, instead of simply reanalyzing all samples in the entire buffer. This is helpful to further reduce the computational overhead.

5 Experiment

Efficiency in RL usually refers to two aspects: *sample efficiency*, the agent’s ability to learn effectively from a limited number of environmental interactions; *time efficiency*, indicated by the wall-clock time taken to achieve a successful policy. **Our primary goal is to improve time efficiency without compromising sample efficiency.**

5.1 Time Efficiency

Setup: To verify the generality of ReZero, we select various decision-making environments and integrate ReZero with different MCTS-based algorithms. **Regarding the environments**, we opt for 26 representative *Atari* environments characterized by classic image-input observation and discrete action spaces, in addition to the strategic board games *Connect4* and *Gomoku* with special state spaces, and two continuous control tasks in *DMControl* [15]. **Regarding the baseline algorithms**, We select three prominent algorithms from the LightZero benchmark [25] as baselines: MuZero with a Self-Supervised Learning loss (SSL), Sampled MuZero and EfficientZero. We integrate ReZero to these algorithms, yielding the enhanced variants ReZero-M, ReZero-SMZ and ReZero-E respectively. When the context is unambiguous, we simply refer to them as ReZero. **Regarding the parameter settings**, we maintain consistent hyper-parameter settings across the algorithms (unless specified cases). Specifically, we set the *replay ratio* (the ratio between environment steps and training steps) [26] to 0.25, and the *reanalyze ratio* (the ratio between targets computed from the environment and by reanalysing existing data) [8] is set to 1. For detailed hyper-parameter configurations, please refer to the Appendix D. Besides, to ensure a fair comparison, all experimental trials were executed on a fixed single worker hardware settings.

Results: Our experiments shown in Figure 4 illustrates the training curves and performance comparisons in terms of wall-clock time between ReZero-M and the MuZero. Note that on the two continuous control tasks we use the ReZero-SMZ and Sampled MuZero [7]. The data clearly indicates that ReZero achieves a significant improvement in time efficiency, attaining a near-optimal policy in significantly less time. We also provide a comparison of the wall-clock training time up to 100k environment steps in Table 1. And we offer the training curves with the environment steps on

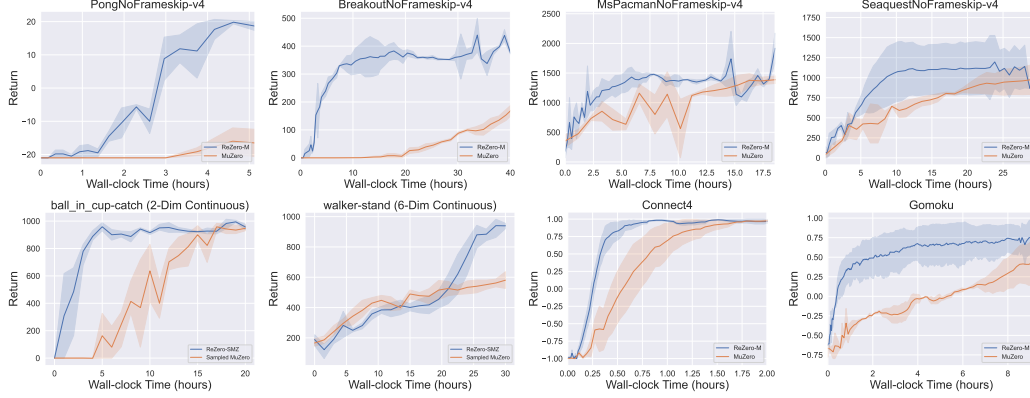


Figure 4: **Time-efficiency** of ReZero-M (ReZero-SMZ) vs. MuZero (Sampled MuZero) on four representative *Atari* games, two continuous control tasks of *DMControl* (*ball_in_cup-catch*, *walker-stand*), and two board games (*Connect4*, *Gomoku*). The horizontal axis represents *Wall-clock Time* (hours), while the vertical axis indicates the *Episode Return* over 5 evaluation episodes. ReZero-M demonstrates superior time-efficiency compared to the baseline across a diverse set of games, encompassing both image and state observations, discrete and continuous actions, and scenarios involving sparse rewards. These figures compute mean of 5 runs, and shaded areas are 95% confidence intervals.

	Atari				DMControl		Board Games	
<i>avg. wall time (h) to 100k env. steps</i> ↓	Pong	Breakout	MsPacman	Seaquest	ball_in_cup-catch	walker-stand	Connect4	Gomoku
ReZero-M (ours)	1.0±0.1	3.0±0.8	1.4±0.2	1.9±0.4	2.1±0.2	4.3±0.3	5.5±0.6	4.5±0.5
MuZero [6]	4.0±0.5	4.9±1.8	6.9±0.3	10.1±0.5	5.6±0.4	9.5±0.6	9.1±0.8	15.3±1.5

Table 1: **Average wall-time** of ReZero-M (ReZero-SMZ) vs. MuZero (Sampled MuZero) on various tasks. (*left*) Four *Atari* games, (*middle*) two control tasks, (*right*) two board games. The time represents the average total wall-time to 100k environment steps for each algorithm. Mean and standard deviation over 5 runs.

the horizontal axis in the Appendix B.4 to show the sample efficiency. These results reveal that, on most games, ReZero require between 2-4 times less wall-clock time per 100k steps compared to the baselines, while maintaining comparable or even superior performance in terms of episode return. Additional results about ReZero-M on 26 *Atari* games and the comparison between ReZero-E and EfficientZero are detailed in the appendix, which can further demonstrate the generality of ReZero in diverse environments and across various algorithms.

6 Conclusion and Limitation

In this paper, we have delved into the efficiency and scalability of MCTS-based algorithms. Unlike most existing works, we incorporate information reuse and periodic reanalyze techniques to reduce wall-clock time costs while preserving sample efficiency. Our theoretical analysis and experimental results confirm that ReZero efficiently reduces the time cost and maintains or even improves performance across different decision-making domains. However, our current experiments are mainly conducted on the single worker setting, there exists considerable optimization scope to apply our approach into distributed RL training, and our design harbors the potential of better parallel acceleration and more stable convergence in large-scale training tasks. Also, the combination between ReZero and frameworks akin to AlphaZero, or its integration with some recent offline datasets such as RT-X [27], constitutes a fertile avenue for future research. These explorations could broaden the application horizons of MCTS-based algorithms. Additionally, since in offline training scenarios, reanalyze becomes the only means of policy improvement, this makes the acceleration of the reanalyze phase in ReZero even more critical. Moreover, the potential improvement in search results by ReZero may further improve the training result, rather than merely accelerating the training. Therefore, combining ReZero with MuZero Unplugged [8] is a direction worth exploring for building foundation models for decision-making.

251 A Proof materials

252 Lemma A: Let w_t be a random variable that satisfies the concentration condition in Equation 2 with
 253 zero expectation, $\varepsilon > 0$, $a > 0$ and

$$\kappa = \sum_{t=1}^n \mathbb{I}\{w_t + \sqrt{\frac{a}{t^2}} \geq \varepsilon\} \quad (9)$$

254 then it holds that $E[\kappa] \leq 1 + \frac{2\sqrt{a}}{\varepsilon} + \frac{C^2}{\varepsilon^2}$.

255 *Proof.* Take u as $\frac{2\sqrt{a}}{\varepsilon}$, then

$$\mathbb{E}[\kappa] \leq u + \sum_{t=\lceil u \rceil}^n \mathbb{P}(w_t + \sqrt{\frac{a}{t^2}} \geq \varepsilon) \quad (10)$$

$$\leq u + \sum_{t=\lceil u \rceil}^n \exp\left(-\frac{t(\varepsilon - \sqrt{\frac{a}{t^2}})^2}{C^2}\right) \quad (11)$$

$$\leq 1 + u + \int_u^\infty \exp\left(-\frac{t(\varepsilon - \sqrt{\frac{a}{t^2}})^2}{C^2}\right) dt \quad (12)$$

$$\leq 1 + u + e^{2\frac{\sqrt{a}\varepsilon}{C^2}} \int_u^\infty e^{-\frac{t\varepsilon^2}{C^2}} dt \quad (13)$$

$$= 1 + u + \frac{C^2}{\varepsilon^2} = 1 + \frac{2\sqrt{a}}{\varepsilon} + \frac{C^2}{\varepsilon^2} \quad (14)$$

256

□

257 Proof for Theorem 1:

258 *Proof.* We first present the upper bound of $\mathbb{E}[T_i(n)]$ for using the Equation 3 in AlphaZero. A slight
 259 adjustment to this proof yields the conclusion of Theorem 1. Denote $T_i(k)$ as the number of times
 260 that arm i has been chosen until time k , A_t as the arm selected at time t , $\hat{\mu}_{is}$ as the average of the
 261 first s samples of arm i , μ_i as the limit of $\mathbb{E}[\hat{\mu}_{is}]$, which satisfies the concentration assumption in
 262 Equation 2, and $\hat{\mu}_i(k) = \hat{\mu}_{iT_i(k)}$. Without loss of generality, we assume that arm 1 is the optimal
 263 arm. Then we have:

$$T_i(n) = \sum_{t=1}^n \mathbb{I}\{A_t = i\} \quad (15)$$

$$\leq \sum_{t=1}^n \mathbb{I}\{\hat{\mu}_1(t-1) + P_1 \frac{\sqrt{t-1}}{1 + T_1(t-1)} \leq \mu_1 - \varepsilon\} \quad (16)$$

$$+ \sum_{t=1}^n \mathbb{I}\{\hat{\mu}_i(t-1) + P_i \frac{\sqrt{t-1}}{1 + T_i(t-1)} \geq \mu_1 - \varepsilon \text{ and } A_t = i\} \quad (17)$$

264 for Equation 16, we have

$$\mathbb{E}[\sum_{t=1}^n \mathbb{I}\{\hat{\mu}_1(t-1) + P_1 \frac{\sqrt{t-1}}{1+T_1(t-1)} \leq \mu_1 - \varepsilon\}] \quad (18)$$

$$\leq 1 + \sum_{t=2}^n \sum_{s=0}^{t-1} \mathbb{P}(\hat{\mu}_{1s} + P_1 \frac{\sqrt{t-1}}{1+s} \leq \mu_1 - \varepsilon) \quad (19)$$

$$= 1 + \sum_{t=2}^n \sum_{s=1}^{t-1} \mathbb{P}(\hat{\mu}_{1s} + P_1 \frac{\sqrt{t-1}}{1+s} \leq \mu_1 - \varepsilon) \quad (20)$$

$$\leq 1 + \sum_{t=2}^n \sum_{s=1}^{t-1} \exp(-\frac{s(\varepsilon + P_1 \frac{\sqrt{t-1}}{1+s})^2}{C^2}) \quad (21)$$

$$\leq 1 + \sum_{t=2}^n \exp(-\frac{1}{C^2} \varepsilon P_1 \sqrt{t-1}) \sum_{s=1}^{t-1} \exp(-\frac{s\varepsilon^2}{C^2}) \quad (22)$$

$$\leq 1 + \sum_{t=2}^n \exp(-\frac{1}{C^2} \varepsilon P_1 \sqrt{t-1}) \frac{C^2}{\varepsilon^2} \quad (23)$$

$$\leq 1 + \frac{2C^6}{\varepsilon^4 P_1^2} \quad (24)$$

265 Notes: In Equation 19, since we assume $P_1 \geq \mu_1$, the probability of the term $s = 0$ would be 0.
 266 Thus, we can discard it. If this assumption doesn't hold, we can choose to accumulate t starting from
 267 a larger t_0 (which satisfies $P_1 \sqrt{t_0 - 1} > \mu_1$ as mentioned in the article). Starting the summation
 268 from such a t_0 ensures all terms of $s = 0$ can still be discarded, and all add terms that $t \leq t_0$ can
 269 be bounded to 1. This only changes the constant term and won't affect the growth rate of regret.
 270 From Equation 21 to Equation 22, we just need to expand the quadratic term and do some simple
 271 inequality scaling. From Equation 22 to Equation 23, we need to notice that $\sum_{s=1}^{t-1} \exp(-\frac{s\varepsilon^2}{C^2})$ is
 272 a geometric sequence and scale it to $\frac{C^2}{\varepsilon^2}$. From Equation 23 to Equation 24, we use the inequality
 273 $\sum_{t=2}^n \frac{1}{e^a \sqrt{t-1}} \leq \int_1^\infty \frac{1}{e^a \sqrt{t-1}}$.

274 And for Equation 17, we have

$$\mathbb{E}[\sum_{t=1}^n \mathbb{I}\{\hat{\mu}_i(t-1) + P_i \frac{\sqrt{t-1}}{1+T_i(t-1)} \geq \mu_1 - \varepsilon \text{ and } A_t = i\}] \quad (25)$$

$$\leq \mathbb{E}[\sum_{t=1}^n \mathbb{I}\{\hat{\mu}_i(t-1) + P_i \sqrt{\frac{n-1}{(1+T_i(t-1))^2}} \geq \mu_1 - \varepsilon \text{ and } A_t = i\}] \quad (26)$$

$$\leq 1 + \mathbb{E}[\sum_{s=1}^{n-1} \mathbb{I}\{\hat{\mu}_{is} + P_i \sqrt{\frac{n-1}{(1+s)^2}} \geq \mu_1 - \varepsilon\}] \quad (27)$$

$$\leq 1 + \mathbb{E}[\sum_{s=1}^n \mathbb{I}\{\hat{\mu}_{is} - \mu_i + P_i \sqrt{\frac{n-1}{s^2}} \geq \Delta_i - \varepsilon\}] \quad (28)$$

275 with Lemma A, we can have

$$28 \leq 2 + \frac{2P_i \sqrt{n-1}}{\Delta_i - \varepsilon} + \frac{C^2}{(\Delta_i - \varepsilon)^2} \quad (29)$$

276 so we have

$$\mathbb{E}[T_i(n)] \leq 3 + \frac{2P_i \sqrt{n-1}}{\Delta_i - \varepsilon} + \frac{C^2}{(\Delta_i - \varepsilon)^2} + \frac{2C^6}{\varepsilon^4 P_1^2} \quad (30)$$

277 The proof of theorem 1 can be obtained by making slight modifications. In case we have drawn n
 278 samples from the same non-stationary distribution as arm 1, and the average of these first n samples
 279 is $\hat{\mu}_1$,

$$\mathbb{E}[T_i(n)] = \mathbb{E}\left[\sum_{t=1}^n \mathbb{I}\{A_t = i\}\right] \quad (31)$$

$$\leq \mathbb{E}\left[\sum_{t=1}^n \mathbb{I}\{\hat{\mu}_1 \leq \mu_1 - \varepsilon\}\right] \quad (32)$$

$$+ \mathbb{E}\left[\sum_{t=1}^n \mathbb{I}\left\{\hat{\mu}_i(t-1) + P_i \frac{\sqrt{t-1}}{1+T_i(t-1)} \geq \mu_1 - \varepsilon \text{ and } A_t = i\right\}\right] \quad (33)$$

$$\leq n \exp\left(-\frac{n\varepsilon^2}{C^2}\right) + \mathbb{E}\left[\sum_{t=1}^n \mathbb{I}\left\{\hat{\mu}_i(t-1) + P_i \frac{\sqrt{t-1}}{1+T_i(t-1)} \geq \mu_1 - \varepsilon \text{ and } A_t = i\right\}\right] \quad (34)$$

$$\leq 2 + \frac{2P_i\sqrt{n-1}}{\Delta_i - \varepsilon} + \frac{C^2}{(\Delta_i - \varepsilon)^2} + n \exp\left(-\frac{n\varepsilon^2}{C^2}\right) \quad (35)$$

280 In case we have drawn n samples from the same non-stationary distribution as arm l , and the average
281 of these first n samples is $\hat{\mu}_l$,

$$\mathbb{E}[T_l(n)] = \mathbb{E}\left[\sum_{t=1}^n \mathbb{I}\{A_t = l\}\right] \quad (36)$$

$$\leq \mathbb{E}\left[\sum_{t=1}^n \mathbb{I}\left\{\hat{\mu}_1(t-1) + P_1 \frac{\sqrt{t-1}}{1+T_1(t-1)} \leq \mu_1 - \varepsilon\right\}\right] \quad (37)$$

$$+ \mathbb{E}\left[\sum_{t=1}^n \mathbb{I}\{\hat{\mu}_l \geq \mu_1 - \varepsilon \text{ and } A_t = l\}\right] \quad (38)$$

$$\leq \mathbb{E}\left[\sum_{t=1}^n \mathbb{I}\left\{\hat{\mu}_1(t-1) + P_1 \frac{\sqrt{t-1}}{1+T_1(t-1)} \leq \mu_1 - \varepsilon\right\}\right] + n \exp\left(-\frac{n(\Delta_l - \varepsilon)^2}{C^2}\right) \quad (39)$$

$$\leq 1 + \frac{2C^6}{\varepsilon^4 P_1^2} + n \exp\left(-\frac{n(\Delta_l - \varepsilon)^2}{C^2}\right) \quad (40)$$

282 and the bound of $E[T_i(n)]$ for $i \neq l$ keeps unchanged. \square

283 B Additional experiments

284 B.1 Effect of Reanalyze Frequency

285 In this section, we adjust the periodic *reanalyze frequency*—which determines how often the buffer
286 is reanalyzed during a training epoch—in ReZero for the *MsPacman* environment. Specifically,
287 we set *reanalyze frequency* to $\{0, \frac{1}{3}, 1, 2\}$. Here, 1 represents the reanalyze frequency we used in
288 the main experiment. The remaining numbers represent setting the frequency to the corresponding
289 multiples. 0 means not using reanalyze at all. The original MuZero with the *reanalyze ratio* of 1
290 is also included in this ablation experiment as a baseline. Figure 5 shows entire training curves in
291 terms of *Wall-time* or *Env Steps* and validates that appropriate reanalyze frequency can save the time
292 overhead without causing any obvious performance loss.

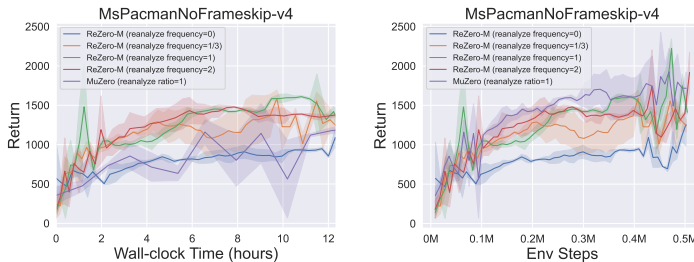


Figure 5: The ablation experiment of **Reanalyze Frequency** in ReZero-M on the *Atari MsPacman* game. The proper reanalyze frequency can improve time and sample efficiency while obtaining the comparable return with MuZero (*reanalyze ratio*=1).

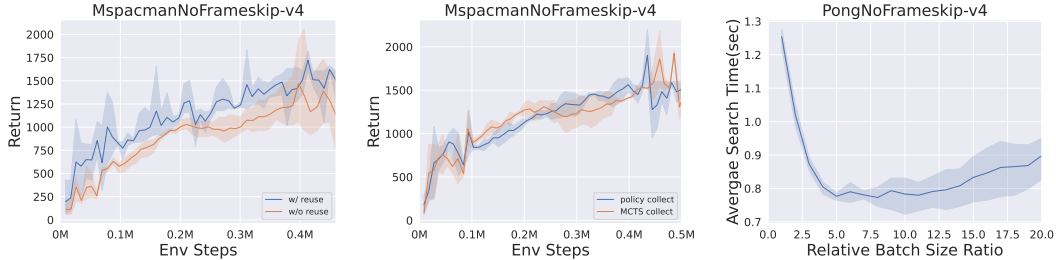
Indicators	Avg. time (ms)	tree search (num calls)	dynamics model (num calls)	data process (num calls)
ReZero-M	0.69 ± 0.02	6089	122	277
MuZero	1.08 ± 0.09	13284	256	455

Table 2: Comparisons about detailed indicators between ReZero-M and MuZero inside the tree search. The number of function calls is the cumulative value of 100 training iterations on *Pong*.

B.2 Effect of Backward-view Reanalyze

To further validate and understand the advantages and significance of the backward-view reanalyze technique proposed in ReZero, we meticulously document a suite of statistical indicators of the tree search process in Table 2. The number of function calls is the cumulative value of 100 training iterations on *Pong*. *Avg. time* is the average time of a MCTS across all calls. Comparative analysis between ReZero-M and MuZero reveals that the backward-view reanalyze technique reduces the invocation frequency of the dynamics model, the search tree, and other operations like data process transformations. Consequently, this advanced technique in leveraging subsequent time step data contributes to save the tree search time in various MCTS-based algorithms, further leading to overall wall-clock time gains. The complexity and implementation of the tree search process directly influences the efficiency gains achieved through the backward-view reanalyze technique. As the tree search becomes more intricate and sophisticated, e.g. Sampled MuZero [7], the time savings realized through this method are correspondingly amplified. Additionally, Theorem 1 demonstrates that the backward-view reanalyze can reduce the regret upper bound, which indicates a better search result. Besides, Figure 6a in Appendix B.3 shows a comparison of sample efficiency between using backward-view reanalyze and origin reanalyze process in *MsPacman*. The experimental results reveal that our method not only enhances the speed of individual searches but also improves sample efficiency. This aligns with the theoretical analysis.

B.3 Additional Ablations



(a) The ablation study comparing the use of backward-view reanalyze versus its absence.

(b) The comparison of sampling actions based on the policy network against using MCTS.

(c) The depiction of the variation in the average search speed of MCTS as the batch size increases.

Figure 6: Additional ablation studies.

This section presents the results of three additional ablation experiments. Figure 6a illustrates the impact of using backward-view reanalyze within the ReZero framework on sample efficiency. The results indicate that backward-view reanalyze, by introducing root value as auxiliary information, achieves higher sample efficiency, aligning with the theoretical analysis regarding regret upper bound. Figure 6b demonstrates the effects of different action selection methods during the collect phase. The findings reveal that sampling actions directly from the distribution output by the policy network does not significantly degrade the experimental results compared to using MCTS for action selection. Figure 6c depicts the relationship between the average MCTS search duration and the batch size. We set a baseline batch size of 256 and experimented with search sizes ranging from 1 to 20 times the baseline, calculating the average time required to search 256 samples by dividing the total search time by the multiplier. The results suggest that larger batch sizes can better leverage the advantages of parallelized model inference and data processing. However, when the batch size be-

comes excessively large, constrained by the limits of hardware resources (memory, CPU), the search speed cannot increase further and may even slightly decrease. We ultimately set the batch size to 2000, which yields the fastest average search speed on our device.

B.4 Sample efficiency

Figure 7 displays the performance over environment interaction steps of the ReZero-M algorithm compared with the original MuZero algorithm across six representative Atari environments and two board games. We can find that ReZero-M obtained *similar* sample efficiency than MuZero on the most tasks.

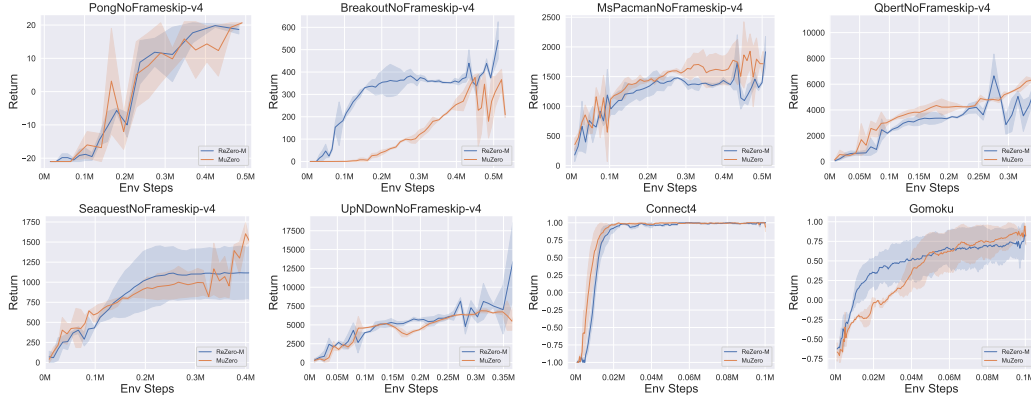


Figure 7: **Sample-efficiency** of ReZero-M vs. MuZero on six representative Atari games and two board games. The horizontal axis represents *Env Steps*, while the vertical axis indicates the *Episode Return* over 5 assessed episodes. ReZero achieves *similar* sample-efficiency than the baseline method. Mean of 5 runs; shaded areas are 95% confidence intervals.

B.5 ReZero-M

In this section, we provide additional experimental results for ReZero-M. As a supplement to Table 1, Table 3 presents the complete experimental results on the 26 Atari environments.

B.6 ReZero-E

The enhancements of ReZero we have proposed are universally applicable to any MCTS-based reinforcement learning approach theoretically. In this section, we integrate ReZero with EfficientZero to obtain the enhanced ReZero-E algorithm. We present the empirical results comparing ReZero-E with the standard EfficientZero across four Atari environments.

Figure 8 shows that ReZero-E is better than EfficientZero in terms of time efficiency. Figure 9 indicates that ReZero-E matches EfficientZero’s sample efficiency across most tasks. Additionally, Table 4 details training times to 100k environment steps, revealing that ReZero-E is significantly faster than baseline methods on most games.

Env. Name	ReZero-M	MuZero
Alien	1.6 ± 0.2	8.6 ± 0.4
Amidar	1.5 ± 0.2	8.1 ± 0.3
Assault	1.5 ± 0.1	7.5 ± 0.1
Asterix	1.3 ± 0.1	7.2 ± 0.2
BankHeist	2.9 ± 0.3	8.9 ± 0.6
BattleZone	2.2 ± 0.3	9.6 ± 0.6
ChopperCommand	3.4 ± 0.4	9.0 ± 0.7
CrazyClimber	2.7 ± 0.1	9.1 ± 0.4
DemonAttack	1.1 ± 0.1	6.8 ± 0.8
Freeway	1.0 ± 0.0	6.1 ± 0.2
Frostbite	2.2 ± 0.4	10.9 ± 0.8
Gopher	3.2 ± 0.6	8.1 ± 0.8
Hero	2.5 ± 0.4	9.9 ± 0.6
Jamesbond	2.2 ± 0.3	9.1 ± 0.5
Kangaroo	2.0 ± 0.2	8.6 ± 0.8
Krull	1.8 ± 0.1	7.7 ± 0.3
KungFuMaster	1.3 ± 0.1	7.6 ± 0.7
PrivateEye	1.0 ± 0.1	5.8 ± 0.5
RoadRunner	1.5 ± 0.2	9.0 ± 0.3
UpNDown	1.4 ± 0.1	7.2 ± 0.4
Pong	1.0 ± 0.1	4.0 ± 0.5
MsPacman	1.4 ± 0.2	6.9 ± 0.3
Qbert	1.3 ± 0.1	7.0 ± 0.3
Seaquest	1.9 ± 0.4	10.1 ± 0.5
Boxing	1.1 ± 0.0	6.6 ± 0.1
Breakout	3.0 ± 0.8	4.9 ± 1.8

Table 3: **Average wall-time**(hours) of ReZero-M vs. MuZero on 26 Atari game environments. The time represents the average total wall-clock time to 100k environment steps. Mean and standard deviation over 5 runs.

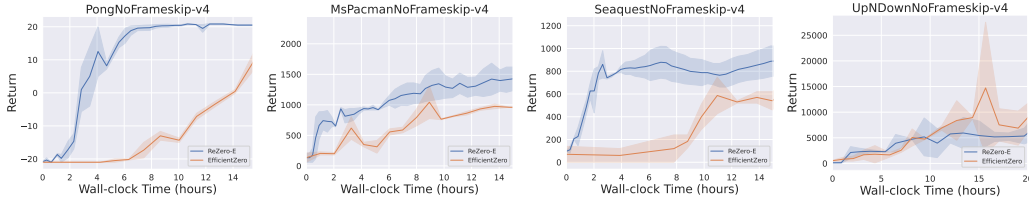


Figure 8: **Time-efficiency** of ReZero-E vs. EfficientZero on four representative Atari games. The horizontal axis represents *Wall-time* (hours), while the vertical axis indicates the *Episode Return* over 5 assessed episodes. ReZero-E achieves higher time-efficiency than the baseline method. Mean of 5 runs; shaded areas are 95% confidence intervals.

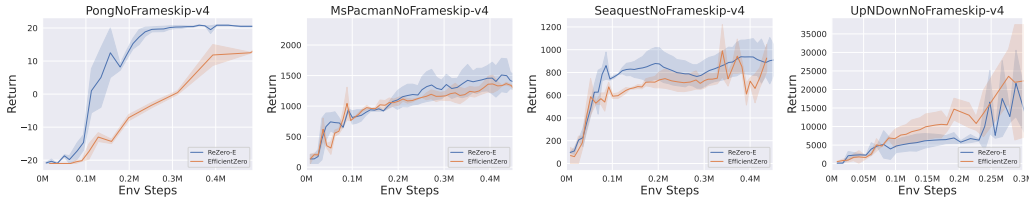


Figure 9: **Sample-efficiency** of ReZero-E vs. EfficientZero on four representative Atari games. The horizontal axis represents *Env Steps*, while the vertical axis indicates the *Episode Return* over 5 assessed episodes. ReZero-E achieves similar sample-efficiency than the baseline method. Mean of 5 runs; shaded areas are 95% confidence intervals.

<i>avg. wall time (h) to 100k env. steps</i> ↓	Pong	MsPacman	Seaquest	UpNDown
ReZero-E (ours)	2.3 ±1.4	3 ±0.3	3.1 ±0.1	3.6 ±0.2
EfficientZero [16]	10±0.2	12±1.3	15±2.3	15±0.7

Table 4: **Average wall-time** of ReZero-E vs. EfficientZero on four Atari games. The time represents the average total wall-time to 100k environment steps for each algorithm. Mean and standard deviation over 5 runs.

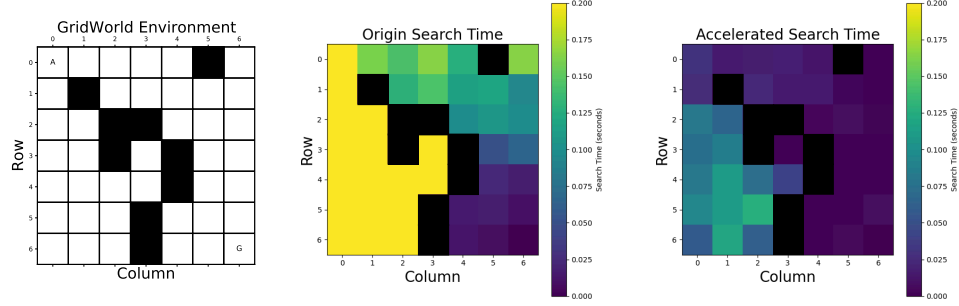


Figure 10: Acceleration effect on the toy case. **Left** is a simple maze environment where the agent starts at point A and receives a reward of size 1 upon reaching the end point G. **Middle** shows the search time corresponding to each position when set as the root node. Meanwhile, the root node values obtained during the search are preserved. **Right** shows the corresponding search time when these root node values are used to assist the search. The comparison shows that the search duration is generally reduced. For specific experimental settings and code, please refer to the Appendix B.7.

B.7 Toy Case

Intuitively, it is evident that our proposed method can achieve a speed gain because we eliminate the search of a certain subtree, especially when this subtree corresponds to the optimal action (which often implies that the subtree has a larger number of nodes). We conduct an experiment on a toy example case. This helps to visually illustrate the speed gain achieved by skipping subtree search and allows readers to quickly understand the algorithm design through simple code. As shown in Figure 10 (Left), we implement a simple 7×7 maze environment where the agent starts at point A and receives a reward of 1 upon reaching point G. We perform an MCTS with each position in the maze as the root node and recorded the search time in Figure 10 (Middle). It can be seen that regions farther from the end point require more time to search (this is related to our simulation settings, see the appendix for details). For comparison, we also performed searches with each position as the root node, but during the search, we used the root node values obtained from the search in Figure 10 (Middle) to evaluate specific actions. The experimental time was recorded in Figure 10 (Right). It can be seen that after eliminating the search of specific subtrees, the search time was generally reduced. This simple result validates the rationality of our algorithm design.

We offer the complete code for the toy case. Readers can compare the core functions `search()` and `reuse_search()` of the MCTS class to understand how root node values are utilized and compare `select()` and `reuse_select()` to understand how the search process is prematurely halted.

```

362 import random
363 import math
364 import time
365 import numpy as np
366 import matplotlib.pyplot as plt
367
368 class Node:
369     def __init__(self, state, parent=None):
370         self.state = state
371         self.parent = parent
372         self.children = []
373         self.visits = 0
374         self.value = 0
375
376     def is_fully_expanded(self):
377         return len(self.children) == len(self.state.get_possible_actions())
378
379     def add_child(self, child_state):
380         child = Node(child_state, self)
381         self.children.append(child)
382         return child
383
384 class MCTS:
385     def __init__(self, exploration_weight=1.0):
386         self.exploration_weight = exploration_weight
387         self.gamma = 0.9
388
389     # the search process in origin MCTS

```

```

391 def search(self, initial_state, max_iter=100):
392     root = Node(initial_state)
393
394     for _ in range(max_iter):
395         node = self.select(root)
396         reward = self.simulate(node.state)
397         self.backpropagate(node, reward)
398
399     best_child = self.get_best_child(root, 0)
400     return best_child.state.current_pos, root.value
401
402 # the search process in our accelerated MCTS by reuse the root value
403 def reuse_search(self, initial_state, value, action, max_iter=100):
404     root = Node(initial_state)
405
406     for _ in range(max_iter):
407         node = self.reuse_select(root, action)
408         if node.state.current_pos == action:
409             reward = value
410         else: reward = self.simulate(node.state)
411         self.backpropagate(node, reward)
412     best_child = self.get_best_child(root, 0)
413     return best_child.state.current_pos, root.value
414
415 # select nodes in origin MCTS
416 def select(self, node):
417     while not node.state.is_terminal():
418         if not node.is_fully_expanded():
419             return self.expand(node)
420         else:
421             node = self.get_best_child(node, self.exploration_weight)
422     return node
423
424 # select nodes in our accelerated MCTS by reuse the root value
425 def reuse_select(self, node, actionpos):
426     while not (node.state.is_terminal() or node.state.current_pos == actionpos):
427         if not node.is_fully_expanded():
428             return self.expand(node)
429         else:
430             node = self.get_best_child(node, self.exploration_weight)
431     return node
432
433 def expand(self, node):
434     actions = node.state.get_possible_actions()
435     for action in actions:
436         if not any(child.state.current_pos == node.state.copy().step(action)[0] for child in node.children):
437             new_state = node.state.copy()
438             new_state.step(action)
439             return node.add_child(new_state)
440     return None
441
442 def simulate(self, state):
443     sim_state = state.copy()
444     count = 1
445     while not sim_state.is_terminal():
446         action = random.choice(sim_state.get_possible_actions())
447         sim_state.step(action)
448         count += 1
449     return sim_state.get_reward()/count
450
451 def backpropagate(self, node, reward):
452     gamma = self.gamma
453     while node is not None:
454         node.visits += 1
455         node.value += reward * gamma
456         node = node.parent
457         gamma *= self.gamma
458
459 def get_best_child(self, node, exploration_weight):
460     best_value = -float('inf')
461     best_children = []
462     for child in node.children:
463         exploit = child.value / child.visits
464         explore = math.sqrt(2.0 * math.log(node.visits) / child.visits)
465         value = exploit + exploration_weight * explore
466         if value > best_value:
467             best_value = value
468             best_children = [child]
469         elif value == best_value:
470             best_children.append(child)
471     return random.choice(best_children)
472
473 class GridWorld:
474     def __init__(self):
475         self.grid = [[0 for _ in range(4)] for _ in range(4)]
476         self.start_pos = (0, 0)
477         self.goal_pos = (0, 3)
478         self.current_pos = self.start_pos
479         self.actions = ['down', 'up', 'left', 'right']

```

```

480
481 def reset(self):
482     self.current_pos = self.start_pos
483     return self.current_pos
484
485 def step(self, action):
486     if action not in self.actions:
487         raise ValueError("Invalid action")
488
489     x, y = self.current_pos
490
491     if action == 'up':
492         x = max(0, x - 1)
493     elif action == 'down':
494         x = min(3, x + 1)
495     elif action == 'left':
496         y = max(0, y - 1)
497     elif action == 'right':
498         y = min(3, y + 1)
499
500     self.current_pos = (x, y)
501     reward = 1 if self.current_pos == self.goal_pos else 0
502     done = self.current_pos == self.goal_pos
503
504     return self.current_pos, reward, done
505
506 def is_terminal(self):
507     return self.current_pos == self.goal_pos
508
509 def get_reward(self):
510     return 1 if self.current_pos == self.goal_pos else 0
511
512 def get_possible_actions(self):
513     x, y = self.current_pos
514     possible_actions = []
515
516     if x > 0:
517         possible_actions.append('up')
518     if x < 3:
519         possible_actions.append('down')
520     if y > 0:
521         possible_actions.append('left')
522     if y < 3:
523         possible_actions.append('right')
524
525     return possible_actions
526
527 def copy(self):
528     new_grid = GridWorld()
529     new_grid.current_pos = self.current_pos
530     return new_grid
531
532 def render(self):
533     for i in range(4):
534         for j in range(4):
535             if (i, j) == self.current_pos:
536                 print("A", end="\n")
537             elif (i, j) == self.goal_pos:
538                 print("G", end="\n")
539             else:
540                 print(".", end="\n")
541         print()
542     print()
543
544 class GridWorldWithWalls:
545     def __init__(self):
546         self.grid = [[0 for _ in range(7)] for _ in range(7)]
547         self.start_pos = (0, 0)
548         self.goal_pos = (6, 6)
549         self.current_pos = self.start_pos
550         self.actions = ['down', 'up', 'left', 'right']
551         self.walls = [(2, 2), (2, 3), (1,1), (3, 2), (3, 4), (3,2), (0,5), (4, 4), (6,3), (5,3)]
552
553         for wall in self.walls:
554             self.grid[wall[0]][wall[1]] = 1
555
556     def reset(self):
557         self.current_pos = self.start_pos
558         return self.current_pos
559
560     def step(self, action):
561         if action not in self.actions:
562             raise ValueError("Invalid action")
563
564         x, y = self.current_pos
565
566         if action == 'up':
567             x = max(0, x - 1)
568         elif action == 'down':

```

```

569         x = min(6, x + 1)
570     elif action == 'left':
571         y = max(0, y - 1)
572     elif action == 'right':
573         y = min(6, y + 1)
574
575     if (x, y) not in self.walls:
576         self.current_pos = (x, y)
577
578     reward = 1 if self.current_pos == self.goal_pos else 0
579     done = self.current_pos == self.goal_pos
580
581     return self.current_pos, reward, done
582
583 def is_terminal(self):
584     return self.current_pos == self.goal_pos
585
586 def get_reward(self):
587     return 1 if self.current_pos == self.goal_pos else 0
588
589 def get_possible_actions(self):
590     x, y = self.current_pos
591     possible_actions = []
592
593     if x > 0 and (x - 1, y) not in self.walls:
594         possible_actions.append('up')
595     if x < 6 and (x + 1, y) not in self.walls:
596         possible_actions.append('down')
597     if y > 0 and (x, y - 1) not in self.walls:
598         possible_actions.append('left')
599     if y < 6 and (x, y + 1) not in self.walls:
600         possible_actions.append('right')
601
602     return possible_actions
603
604 def copy(self):
605     new_grid = GridWorldWithWalls()
606     new_grid.current_pos = self.current_pos
607     return new_grid
608
609 def render(self):
610     for i in range(7):
611         for j in range(7):
612             if (i, j) == self.current_pos:
613                 print("A", end=" ")
614             elif (i, j) == self.goal_pos:
615                 print("G", end=" ")
616             elif (i, j) in self.walls:
617                 print("#", end=" ")
618             else:
619                 print(".", end=" ")
620         print()
621     print()
622
623 env = GridWorldWithWalls()
624 mcts = MCTS()
625
626 # plot the grid
627 plt.figure(figsize=(6, 6))
628 plt.matshow(env.grid, cmap='binary', fignum=0, vmin=0, vmax=1)
629
630 for i in range(7):
631     for j in range(7):
632         if (i, j) == env.start_pos:
633             plt.text(j, i, 'A', ha='center', va='center', color='black', fontsize=12)
634         elif (i, j) == env.goal_pos:
635             plt.text(j, i, 'G', ha='center', va='center', color='black', fontsize=12)
636         elif (i, j) in env.walls:
637             plt.text(j, i, '#', ha='center', va='center', color='black', fontsize=12)
638         else:
639             plt.text(j, i, '.', ha='center', va='center', color='black', fontsize=12)
640
641 for wall in env.walls:
642     plt.gca().add_patch(plt.Rectangle((wall[1] - 0.5, wall[0] - 0.5), 1, 1, color='black'))
643
644 for i in range(7):
645     for j in range(7):
646         plt.gca().add_patch(plt.Rectangle((j - 0.5, i - 0.5), 1, 1, fill=False, edgecolor='black', linewidth=2))
647
648 plt.title('GridWorld Environment', fontsize=24)
649 plt.xticks(np.arange(7), ['0', '1', '2', '3', '4', '5', '6'])
650 plt.yticks(np.arange(7), ['0', '1', '2', '3', '4', '5', '6'])
651 plt.xlabel('Column', fontsize=24)
652 plt.ylabel('Row', fontsize=24)
653 plt.show()
654
655 # record the search time
656 search_times = np.zeros((7, 7))

```

```

658 reuse_times = np.zeros((7, 7))
659 for i in range(7):
660     for j in range(7):
661         if (i, j) == env.goal_pos or (i, j) in env.walls:
662             continue
663
664         env.current_pos = (i, j)
665         print(f"Starting_MCTS_from_position:{env.current_pos}")
666
667         start_time = time.time()
668         reuse_action, root_value = mcts.search(env)
669         end_time = time.time()
670         search_time = end_time - start_time
671         search_times[i, j] = search_time
672
673         env.current_pos = reuse_action
674         if reuse_action == env.goal_pos:
675             reuse_value = 1
676         else: _, reuse_value = mcts.search(env)
677
678         env.current_pos = (i, j)
679         start_time = time.time()
680         best_action, root_value = mcts.reuse_search(env, reuse_value, reuse_action)
681         end_time = time.time()
682         reuse_time = end_time - start_time
683         reuse_times[i, j] = reuse_time
684
685
686         print(f"Best_action_leads_to_position:{reuse_action}")
687         print(f"Reuse_search_best_action_leads_to_position:{best_action}")
688         print(f"Search_time:{search_time:.4f}seconds")
689         print(f"reuseSearch_time:{reuse_time:.4f}seconds\n")
690
691 # plot the time heatmap
692 plt.figure(figsize=(6, 6))
693 plt.imshow(search_times, cmap='viridis', vmin=0, vmax=0.2, interpolation='nearest')
694 plt.colorbar(label='Search_Time(seconds)')
695 plt.title('Origin_Search_Time', fontsize=20)
696 plt.xticks(np.arange(7), ['0', '1', '2', '3', '4', '5', '6'])
697 plt.yticks(np.arange(7), ['0', '1', '2', '3', '4', '5', '6'])
698 plt.xlabel('Column', fontsize=20)
699 plt.ylabel('Row', fontsize=20)
700 plt.figure(figsize=(6, 6))
701 plt.imshow(reuse_times, cmap='viridis', vmin=0, vmax=0.2, interpolation='nearest')
702 plt.colorbar(label='Search_Time(seconds)')
703 plt.title('Accelerated_Search_Time', fontsize=20)
704 plt.xticks(np.arange(7), ['0', '1', '2', '3', '4', '5', '6'])
705 plt.yticks(np.arange(7), ['0', '1', '2', '3', '4', '5', '6'])
706 plt.xlabel('Column', fontsize=20)
707 plt.ylabel('Row', fontsize=20)
708 plt.show()
709

```

C MuZero

During the *inference* phase, the representation model transforms a sequence of the last l observations $o_{t-l:t}$ into a corresponding latent state representation s_t . The dynamics model processes this latent state alongside an action a_t , yielding the subsequent latent state s_{t+1} and an estimated reward r_t . Finally, the prediction model accepts a latent state and produces both the predicted policy p_t and the state's value estimate v_t . These outputs are instrumental in guiding the agent's action selection process throughout its MCTS. Lastly the agent selects or samples the best action a_t following the searched visit count distribution. During the *training* phase, given a training sequence $\{o_{t-l:t+K}, a_{t+1:t+K}, u_{t+1:t+K}, \pi_{t+1:t+K}, z_{t+1:t+K}\}$ at time t sampled from the replay buffer, where u_{t+k} denotes the actual reward obtained from the environment, π_{t+k} represents the target policy obtained through MCTS during the agent-environment interaction, and z_{t+k} is the value target computed using n -step *bootstrapping* [28]. The representation model initially converts the sequence of observations $o_{t-l:t}$ into the latent state s_t^0 . Subsequently, the dynamic model executes K latent space rollouts based on the sequence of actions $a_{t+1:t+K}$. The latent state derived after the k -th rollout is denoted as s_t^k , with the corresponding predicted reward indicated as r_t^k . Upon receiving s_t^k , the prediction model generates a predicted policy p_t^k and a estimated value v_t^k . The final training loss encompasses three components: the policy loss (l_p), the value loss (l_v), and the reward loss (l_r):

$$L_{\text{MuZero}} = \sum_{k=0}^K l_p(\pi_{t+k}, p_t^k) + \sum_{k=0}^K l_v(z_{t+k}, v_t^k) + \sum_{k=1}^K l_r(u_{t+k}, r_t^k) \quad (41)$$

MuZero *Reanalyze*, as introduced in [8], is an advanced iteration of the original MuZero algorithm. This variant enhances the model’s accuracy by conducting a fresh Monte Carlo Tree Search on sampled states with the most recent version of the model, subsequently utilizing the refined policy from this search to update the policy targets. Such reanalysis yields targets of superior quality compared to those obtained during the initial data collection phase. The Schrittwieser et al. [8] expands upon this approach, formalizing it as a standalone method for policy refinement. This innovation opens avenues for its application in offline settings, where interactions with the environment are not possible.

D Implementation details

D.1 Environments

In this section, we first introduce various types of reinforcement learning environments evaluated in the main paper and their respective characteristics, including different observation/action/reward space and transition functions.

Atari: This category includes sub-environments like *Pong*, *Qbert*, *Ms.Pacman*, *Breakout*, *UpN-Down*, and *Seaquest*. In these environments, agents control game characters and perform tasks based on pixel input, such as hitting bricks in *Breakout*. With their high-dimensional visual input and discrete action space features, Atari environments are widely used to evaluate the capability of reinforcement learning algorithms in handling visual inputs and discrete control problems.

DMControl: This continuous control suite comprises 39 continuous control tasks. Our focus here is to validate the effectiveness of ReZero in the continuous action space. Consequently, we have utilized two representative tasks (*ball_in_cup-catch* and *walker-stand*) for illustrative purposes. A comprehensive benchmark for this domain will be included in future versions.

Board Games: This types of environment includes *Connect4*, *Gomoku*, where uniquely marked boards and explicitly defined rules for placement, movement, positioning, and attacking are employed to achieve the game’s ultimate objective. These environments feature a variable discrete action space, allowing only one player’s piece per board position. In practice, algorithms utilize action mask to indicate reasonable actions.

D.2 Algorithm Implementation Details

Our algorithm’s implementation is based on the open-source code of LightZero [25]. Given that our proposed theoretical improvements are applicable to any MCTS-based RL method, we have chosen MuZero and EfficientZero as case studies to investigate the practical improvements in time efficiency achieved by integrating the ReZero boosting techniques: *just-in-time reanalyze* and *speedy reanalyze* (*temporal information reuse*).

To ensure an equitable comparison of wall-clock time, all experimental trials were executed on a fixed single worker hardware setting consisting of a single NVIDIA A100 GPU with 30 CPU cores and 120 GiB memory. Besides, we emphasize that to ensure a fair comparison of time efficiency and sample efficiency, the model architecture and hyper-parameters used in the experiments of Section 5 are essentially consistent with the settings in LightZero. For specific hyper-parameters of *ReZero-M* and *MuZero* on Atari, please refer to the Table 7. The main different hyper-parameters in the *DMControl* task are set out in Tables 5. The main different hyper-parameters for the *ReZero-M* algorithm in the *Connect4* and *Gomoku* environment are set out in Tables 6. In addition to employing an LSTM network with a hidden state dimension of 512 to predict the value prefix [16], all hyperparameters of ReZero-E are essentially identical to those of ReZero-M in Table 7.

Hyperparameter	Value
Replay ratio [30]	0.25
Reanalyze frequency	1
Batch size	64
Num of frames stacked	1
Num of frames skip	2
Discount factor	0.997
Length of game segment	8
Use augmentation	False
Number of simulations in MCTS (sim)	50
Number of sampled actions [7]	20

Table 5: Key hyperparameters of **ReZero-M** on two *DMControl* tasks (*ball_in_cup-catch* and *walker-stand*). More experiments about this hyper-parameter will be explored in the future version. Other unmentioned parameters are the same as that in *Atari* settings.

771 **Wall-time statistics** Note that all our current tests are conducted in the single-worker case. There-
772 fore, the wall-time reported in Table 1 and Table 4 for reaching 100k env steps includes:

- 773 • *collect time*: The total time spent by an agent interacting with the environment to gather experience
774 data. Weng et al. [9] can be integrated to speed up. Besides, this design also makes MCTS-based
775 algorithms compatible to existing RL exploration methods like Burda et al. [29].
- 776 • *reanalyze time*: The time used to reanalyze collected data with the current policy or value function
777 for more accurate learning targets [8].
- 778 • *train time*: The duration for performing updates to the agent’s policy, value functions and model
779 based on collected data.
- 780 • *evaluation time*: The period during which the agent’s policy is tested against the environment,
781 separate from training, to assess performance.

782 Currently, we have set *collect_max_episode_steps* to 10,000 and *eval_max_episode_steps* to 20,000
783 to mitigate the impact of anomalously long evaluation episodes on time. In the future, we will con-
784 sider conducting offline evaluations to avoid the influence of evaluation time on our measurement of
785 time efficiency. Furthermore, the ReZero methodology represents a pure algorithmic enhancement,
786 eliminating the need for supplementary computational resources or additional overhead. This ap-
787 proach is versatile, enabling seamless integration with single-worker serial execution environments
788 as well as multi-worker asynchronous frameworks. The exploration of ReZero’s extensions and its
789 evaluations in a multi-worker [10] paradigm are earmarked for future investigation.

790 **Board games settings** Given that our primary objective is to test the proposed techniques for im-
791 provements in time efficiency, we consider a simplified version of single-player mode in all the
792 board games. This involves setting up a fixed but powerful expert bot and treating this opponent
793 as an integral part of the environment. Exploration of our proposed techniques in the context of
794 learning through self-play training pipeline is reserved for our future work.

Hyperparameter	Value
Replay ratio [30]	0.25
Reanalyze frequency	1
Board size	6x7; 6x6
Num of frames stacked	1
Discount factor	1
Weight of SSL (self-supervised learning) loss	0
Length of game segment	18
TD steps	21; 18
Use augmentation	False
Number of simulations in MCTS (sim)	50
The scale of supports used in categorical distribution	10

Table 6: Key hyperparameters of **ReZero-M** on *Connect4* and *Gomoku* environments. If the parameter settings of these two environments are different, they are separated by a semicolon.

Hyperparameter	Value
Replay Ratio [30]	0.25
Reanalyze frequency	1
Num of frames stacked	4
Num of frames skip	4
Reward clipping [23]	True
Optimizer type	Adam
Learning rate	3×10^{-3}
Discount factor	0.997
Weight of policy loss	1
Weight of value loss	0.25
Weight of reward loss	1
Weight of policy entropy loss	0
Weight of SSL (self-supervised learning) loss [16]	2
Batch size	256
Model update ratio	0.25
Frequency of target network update	100
Weight decay	10^{-4}
Max gradient norm	10
Length of game segment	400
Replay buffer size (in transitions)	1e6
TD steps	5
Number of unroll steps	5
Use augmentation	True
Discrete action encoding type	One Hot
Normalization type	Layer Normalization
Priority exponent coefficient [31]	0.6
Priority correction coefficient	0.4
Dirichlet noise alpha	0.3
Dirichlet noise weight	0.25
Number of simulations in MCTS (sim)	50
Categorical distribution in value and reward modeling	True
The scale of supports used in categorical distribution [32]	300

Table 7: Key hyperparameters of **ReZero-M** on *Atari* environments.

References

- [1] M. Janner, J. Fu, M. Zhang, and S. Levine. When to trust your model: Model-based policy optimization. *Advances in neural information processing systems*, 32, 2019.
- [2] D. Hafner, T. Lillicrap, M. Norouzi, and J. Ba. Mastering atari with discrete world models. *arXiv preprint arXiv:2010.02193*, 2020.
- [3] M. Świechowski, K. Godlewski, B. Sawicki, and J. Mańdziuk. Monte carlo tree search: A review of recent modifications and applications. *Artificial Intelligence Review*, 56(3):2497–2562, 2023.
- [4] P. Auer, N. Cesa-Bianchi, and P. Fischer. Finite-time analysis of the multiarmed bandit problem. *Machine learning*, 47:235–256, 2002.
- [5] D. Silver, T. Hubert, J. Schrittwieser, I. Antonoglou, M. Lai, A. Guez, M. Lanctot, L. Sifre, D. Kumaran, T. Graepel, et al. Mastering chess and shogi by self-play with a general reinforcement learning algorithm. *arXiv preprint arXiv:1712.01815*, 2017.
- [6] J. Schrittwieser, I. Antonoglou, T. Hubert, K. Simonyan, L. Sifre, S. Schmitt, A. Guez, E. Lockhart, D. Hassabis, T. Graepel, T. P. Lillicrap, and D. Silver. Mastering atari, go, chess and shogi by planning with a learned model. *CoRR*, abs/1911.08265, 2019. URL <http://arxiv.org/abs/1911.08265>.
- [7] T. Hubert, J. Schrittwieser, I. Antonoglou, M. Barekatin, S. Schmitt, and D. Silver. Learning and planning in complex action spaces. In M. Meila and T. Zhang, editors, *Proceedings of the 38th International Conference on Machine Learning, ICML 2021, 18-24 July 2021, Virtual Event*, volume 139 of *Proceedings of Machine Learning Research*, pages 4476–4486. PMLR, 2021. URL <http://proceedings.mlr.press/v139/hubert21a.html>.
- [8] J. Schrittwieser, T. Hubert, A. Mandhane, M. Barekatin, I. Antonoglou, and D. Silver. Online and offline reinforcement learning by planning with a learned model. *Advances in Neural Information Processing Systems*, 34:27580–27591, 2021.
- [9] J. Weng, M. Lin, S. Huang, B. Liu, D. Makoviychuk, V. Makoviychuk, Z. Liu, Y. Song, T. Luo, Y. Jiang, et al. Envpool: A highly parallel reinforcement learning environment execution engine. *Advances in Neural Information Processing Systems*, 35:22409–22421, 2022.
- [10] Y. Mei, J. Gao, W. Ye, S. Liu, Y. Gao, and Y. Wu. Speedyzero: Mastering atari with limited data and time. In *The Eleventh International Conference on Learning Representations*, 2023.
- [11] Y. Fu, M. Sun, B. Nie, and Y. Gao. Accelerating monte carlo tree search with probability tree state abstraction. *arXiv preprint arXiv:2310.06513*, 2023.
- [12] T. Lattimore and C. Szepesvári. *Bandit algorithms*. Cambridge University Press, 2020.
- [13] M. G. Bellemare, Y. Naddaf, J. Veness, and M. Bowling. The arcade learning environment: An evaluation platform for general agents. *Journal of Artificial Intelligence Research*, 47: 253–279, 2013.
- [14] D. Silver, A. Huang, C. J. Maddison, A. Guez, L. Sifre, G. Van Den Driessche, J. Schrittwieser, I. Antonoglou, V. Panneershelvam, M. Lanctot, et al. Mastering the game of go with deep neural networks and tree search. *nature*, 529(7587):484–489, 2016.
- [15] S. Tunyasuvunakool, A. Muldal, Y. Doron, S. Liu, S. Bohez, J. Merel, T. Erez, T. Lillicrap, N. Heess, and Y. Tassa. dm control: Software and tasks for continuous control. *Software Impacts*, 6:100022, 2020. ISSN 2665-9638. doi:<https://doi.org/10.1016/j.simpa.2020.100022>. URL <https://www.sciencedirect.com/science/article/pii/S2665963820300099>.

- [16] W. Ye, S. Liu, T. Kurutach, P. Abbeel, and Y. Gao. Mastering atari games with limited data. *Advances in Neural Information Processing Systems*, 34:25476–25488, 2021.
- [17] I. Antonoglou, J. Schrittwieser, S. Ozair, T. K. Hubert, and D. Silver. Planning in stochastic environments with a learned model. In *International Conference on Learning Representations*, 2021.
- [18] I. Danihelka, A. Guez, J. Schrittwieser, and D. Silver. Policy improvement by planning with gumbel. In *International Conference on Learning Representations*, 2022.
- [19] D. J. Wu. Accelerating self-play learning in go. *arXiv preprint arXiv:1902.10565*, 2019.
- [20] E. Leurent and O.-A. Maillard. Monte-carlo graph search: the value of merging similar states. In *Asian Conference on Machine Learning*, pages 577–592. PMLR, 2020.
- [21] C. Grimm, A. Barreto, S. Singh, and D. Silver. The value equivalence principle for model-based reinforcement learning. *Advances in Neural Information Processing Systems*, 33:5541–5552, 2020.
- [22] L. Kocsis and C. Szepesvári. Bandit based monte-carlo planning. In *European conference on machine learning*, pages 282–293. Springer, 2006.
- [23] V. Mnih, K. Kavukcuoglu, D. Silver, A. Graves, I. Antonoglou, D. Wierstra, and M. Riedmiller. Playing atari with deep reinforcement learning. *arXiv preprint arXiv:1312.5602*, 2013.
- [24] A. P. Badia, P. Sprechmann, A. Vitvitskyi, D. Guo, B. Piot, S. Kapturowski, O. Tieleman, M. Arjovsky, A. Pritzel, A. Bolt, et al. Never give up: Learning directed exploration strategies. *arXiv preprint arXiv:2002.06038*, 2020.
- [25] Y. Niu, Y. Pu, Z. Yang, X. Li, T. Zhou, J. Ren, S. Hu, H. Li, and Y. Liu. Lightzero: A unified benchmark for monte carlo tree search in general sequential decision scenarios. *arXiv preprint arXiv:2310.08348*, 2023.
- [26] P. D’Oro, M. Schwarzer, E. Nikishin, P.-L. Bacon, M. G. Bellemare, and A. Courville. Sample-efficient reinforcement learning by breaking the replay ratio barrier. In *Deep Reinforcement Learning Workshop NeurIPS 2022*, 2022.
- [27] A. Padalkar, A. Pooley, A. Jain, A. Bewley, A. Herzog, A. Irpan, A. Khazatsky, A. Rai, A. Singh, A. Brohan, et al. Open x-embodiment: Robotic learning datasets and rt-x models. *arXiv preprint arXiv:2310.08864*, 2023.
- [28] M. Hessel, J. Modayil, H. Van Hasselt, T. Schaul, G. Ostrovski, W. Dabney, D. Horgan, B. Piot, M. Azar, and D. Silver. Rainbow: Combining improvements in deep reinforcement learning. In *Proceedings of the AAAI conference on artificial intelligence*, volume 32, 2018.
- [29] Y. Burda, H. Edwards, A. Storkey, and O. Klimov. Exploration by random network distillation. *arXiv preprint arXiv:1810.12894*, 2018.
- [30] M. Schwarzer, J. S. O. Ceron, A. Courville, M. G. Bellemare, R. Agarwal, and P. S. Castro. Bigger, better, faster: Human-level atari with human-level efficiency. In *International Conference on Machine Learning*, pages 30365–30380. PMLR, 2023.
- [31] T. Schaul, J. Quan, I. Antonoglou, and D. Silver. Prioritized experience replay. *arXiv preprint arXiv:1511.05952*, 2015.
- [32] T. Pohlen, B. Piot, T. Hester, M. G. Azar, D. Horgan, D. Budden, G. Barth-Maron, H. Van Hasselt, J. Quan, M. Večerík, et al. Observe and look further: Achieving consistent performance on atari. *arXiv preprint arXiv:1805.11593*, 2018.